===================== **MAGNETISM** =====================

Magnetic and Natural Optical Activity of *f–f* Transitions in Multiferroic $Nd_{0.5}Gd_{0.5}Fe_3(BO_3)_4$

A. V. Malakhovskii*, A. L. Sukhachev, A. A. Leont'ev, and V. L. Temerov

Kirensky Institute of Physics, Siberian Branch, Russian Academy of Sciences,
Akademgorodok 50/38, Krasnoyarsk, 660036 Russia
*e-mail: malakha@iph.krasn.ru
Received October 13, 2015

Abstract—Spectra of absorption, magnetic circular dichroism, and natural circular dichroism of the *f–f* transitions $^4I_{9/2} \rightarrow {^4F_{3/2}}$, $^2H_{9/2} + {^4F_{5/2}}$, $^4S_{3/2} + {^4F_{7/2}}$, $^2G_{7/2} + {^4G_{5/2}}$, $^2K_{13/2} + {^4G_{7/2}}$, and $^4G_{9/2}$ in the Nd^{3+} ions in the $Nd_{0.5}Gd_{0.5}Fe_3(BO_3)_4$ crystal have been measured as a function of the temperature in the interval of 90–300 K. Temperature dependences of the magneto-optical activity (MOA) and natural optical activity (NOA) of the transitions have been obtained. It has been found that, in contrast to allowed transitions, the temperature dependence of the MOA of the *f–f* transitions does not obey the Curie−Weiss law and the NOA depends on temperature. The NOA of some transitions changes the sign with variation in temperature. These phenomena have been explained by the presence of three contributions to the allowance of the *f–f* transitions, which lead to three contributions of different signs to the MOA and NOA. The range of the MOA of the *f–f* transitions in the Nd^{3+} ion has been predicted theoretically and confirmed experimentally.

1. INTRODUCTION

There are many works devoted to the magnetic circular dichroism (MCD) of parity-forbidden *f–f* transitions (see, e.g., [1−7]), including those in neodymium compounds [2, 3, 6]. In most of these works, the MCD was measured only at one or a few temperatures and the analysis consisted in the decomposition of the MCD into the paramagnetic and diamagnetic parts. In our works (e.g., [8−12]), for the first time, temperature dependences of the integral paramagnetic magneto-optical activity (MOA) of the *f–f* transitions were studied and theoretically explained. In particular, it was shown that the behavior and value of the MOA of the *f–f* transitions are directly connected with the nature of the allowance of these transitions. This work is devoted to similar studies in the $Nd_{0.5}Gd_{0.5}Fe_3(BO_3)_4$ crystal. We also studied the temperature dependences of the integral natural optical activity (NOA) of the *f–f* transitions in this crystal. Measurements of the NOA of the *f–f* transitions are more rare than measurements of the MOA (see, e.g., [13−18] and references therein) and temperature dependences of the NOA of the *f–f* transitions were measured for the first time in our work devoted to the $ErAl_3(BO_3)_4$ crystal [8]. In contrast to the MOA, the NOA is more sensitive to local distortions in the excited states of the 4*f* ion. The $Nd_{0.5}Gd_{0.5}Fe_3(BO_3)_4$ crystal, as well as purely neodymium and gadolinium ferroborates, is multiferroic [19], i.e., possesses mutu-ally dependent magnetic and electric polarizations. The magnetic properties of the $Nd_{0.5}Gd_{0.5}Fe_3(BO_3)_4$ crystal were studied in [20]. Below $T_N = 32$ K, the crystal becomes an easy-plane antiferromagnet and remains in this state at least down to 2 K. In the paramagnetic region, it is characterized by two Weiss parameters: along the third-order axis, $\theta_C = -45$ K and, in the basis plane, $\theta_{ab} = -70$ K. At room temperature, the $Nd_{0.5}Gd_{0.5}Fe_3(BO_3)_4$ crystal has the huntite structure with the trigonal spatial symmetry $R32 (D_3^7)$ and the unit cell parameters $a = 9.557(7)$ Å and $c = 7.62(1)$ Å. The structural phase transition is not detected down to 2 K [20]. The unit cell contains three formula units. Rare-earth ions are found at the centers of trigonal prisms RO_6 (local symmetry D_3). Fe^{3+} ions occupy the C_2-positions in the octahedral environment of oxygen ions. These octahedra form helical chains along the axis C_3.

The Judd−Ofelt spectroscopic parameters of the $Nd_{0.5}Gd_{0.5}Fe_3(BO_3)_4$ crystal were determined in [21] and, in [22, 23], selection rules for the *f–f* transitions and the local properties in excited 4*f* electron states in the magnetically ordered crystal were studied.

2. EXPERIMENT

$Nd_{0.5}Gd_{0.5}Fe_3(BO_3)_4$ single crystals were grown from a solution−melt based on $K_2Mo_3O_{10}$ by the
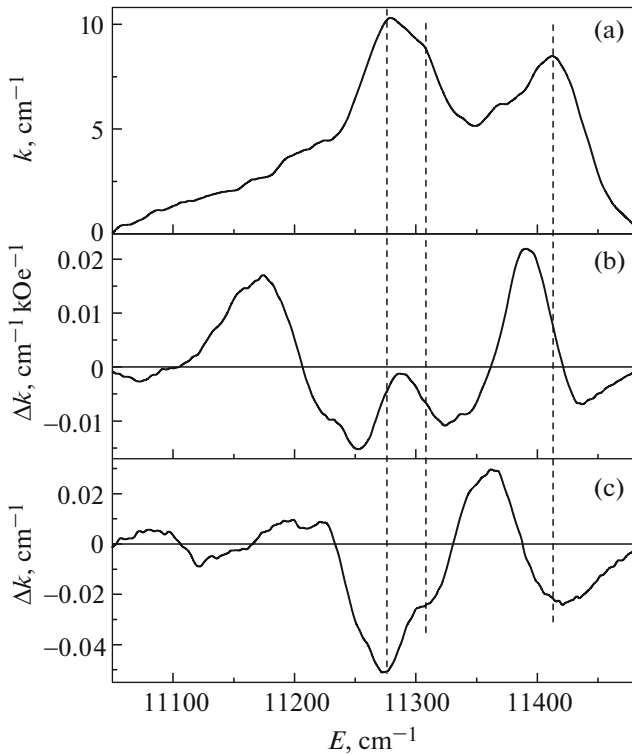
Fig. 1. (a) Absorption, (b) MCD, and (c) NCD spectra of the $^4I_{9/2} \rightarrow {}^4F_{3/2}$ transition (R-band) at room temperature.
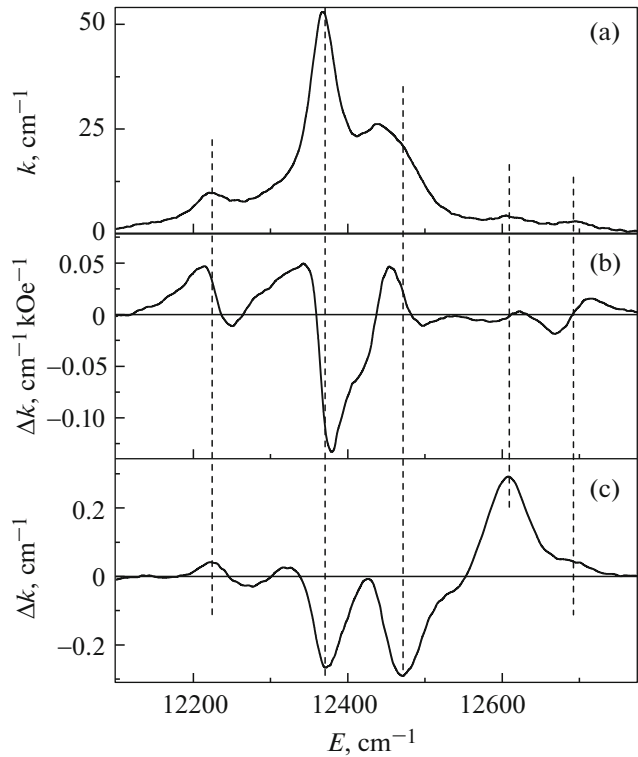
Fig. 2. (a) Absorption, (b) MCD, and (c) NCD spectra of the $^4I_{9/2} \rightarrow {}^2H_{9/2} + {}^4F_{5/2}$ transition (S-band) at room temperature.

method described in [24]. Samples were cut perpendicularly to axis C_3 of the crystal. The absorption spectra were obtained on an automatic double beam spectrophotometer on the basis of the MDR-2 monochromator.

The circular dichroism was measured by modulation of the circular polarization with a piezoelectric modulator [23]. The MCD was obtained as the half-difference of the circular dichroisms in opposite magnetic fields, and the natural circular dichroism (NCD) was obtained as the half-sum of these values. The measurements were performed in a field of 5 kOe. The sensitivity of the dichrograph for measuring the circular dichroism was ~10^{-4}. The spectra and circular dichroism spectra were measured in α-polarized light, i.e., in light propagating along the trigonal axis C_3 of the crystal. The optical band width in all measurements was 0.2 nm in the band 450–600 nm and, 0.4 nm, in the range of 600–1000 nm. The sample was placed in a nitrogen gas continuous-flow cryostat. The temperature was maintained in the range of 90–293 K with an accuracy of ~1 K.

3. RESULTS AND DISCUSSION

The absorption spectrum of the $Nd_{0.5}Gd_{0.5}Fe_3(BO_3)_4$ crystal consists of narrow bands

corresponding to the f–f transitions in the Nd^{3+} ion and wide bands caused by the d–d transitions in the Fe^{3+} ion [23]. The absorption, MCD, and NCD spectra were measured in the frequency range of 10000–22000 cm^{-1}. From the high-energy side, they are bounded by strong Fe–Fe charge-transfer transitions (the Mott–Hubbard transitions) [25]. The spectra of the d–d transitions were approximated by Gaussian curves and subtracted from the total spectra. The circular dichroism spectra caused by the d–d transitions were not observed. The absorption, MCD, and NCD spectra of all f–f transitions under study: $^4I_{9/2} \rightarrow {}^4F_{3/2}$ (R), $^2H_{9/2} + {}^4F_{5/2}$ (S), $^4S_{3/2} + {}^4F_{7/2}$ (A), $^2G_{7/2} + {}^4G_{5/2}$ (D), $^2K_{13/2} + {}^4G_{7/2}$ (E), and $^4G_{9/2}$ (F) at room temperature are presented in Figs. 1–5. The temperature dependences of the integral intensities of the absorption bands are demonstrated in Fig. 6. In [23], it was shown that the f–f absorption in the crystal has an electric-dipole character.

The MCD of the Zeeman doublet is described by the relationship [9]

$$\Delta k = k_m c \varphi(\omega, \omega_0) + k_m \Delta \omega_0 \partial \varphi(\omega, \omega_0)/\partial \omega_0. \quad (1)$$

The first term in (1) is the paramagnetic MCD, the second term is the diamagnetic MCD, $k_m = k_{m+} + k_{m-}$ is the amplitude of the line not split by the magnetic
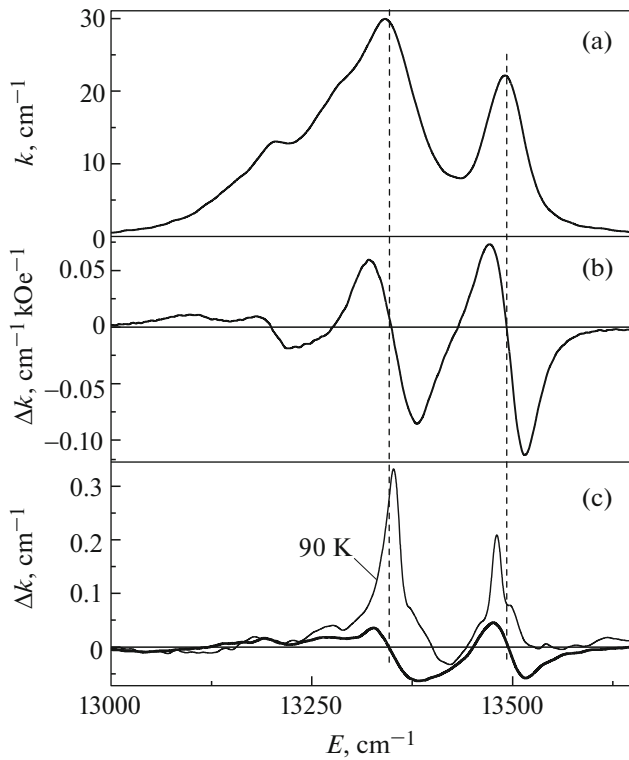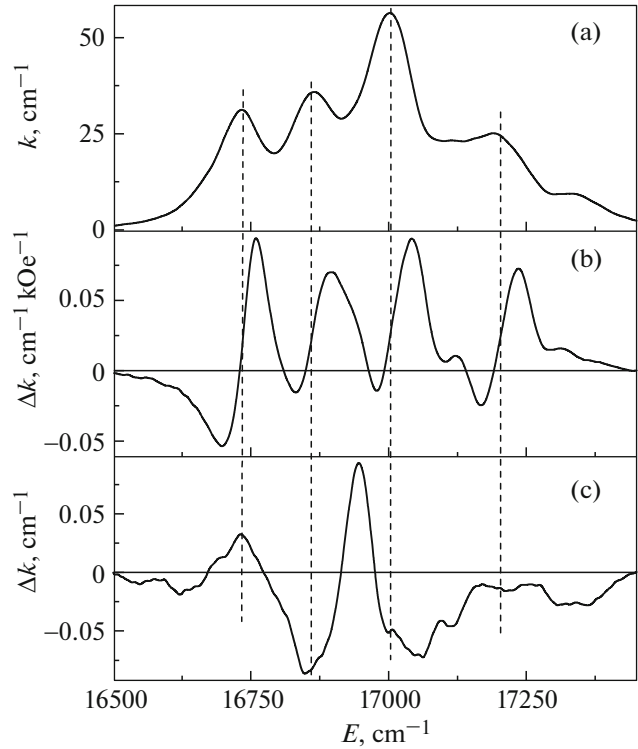
Fig. 3. (a) Absorption, (b) MCD, and (c) NCD spectra of the $^4I_{9/2} \rightarrow {}^4S_{3/2} + {}^4F_{7/2}$ transition (A-band) at room temperature. For NCD, the NCD spectrum at 90 K is also presented.

Fig. 4. (a) Absorption, (b) MCD, and (c) NCD spectra of the $^4I_{9/2} \rightarrow {}^2G_{7/2} + {}^4G_{5/2}$ transition (D-band) at room temperature.

Fig. 5. (a) Absorption, (b) MCD, and (c) NCD spectra of the $^4I_{9/2} \rightarrow {}^2K_{13/2} + {}^4G_{7/2}$ and $^4G_{9/2}$ transitions (E- and F-bands) at room temperature.
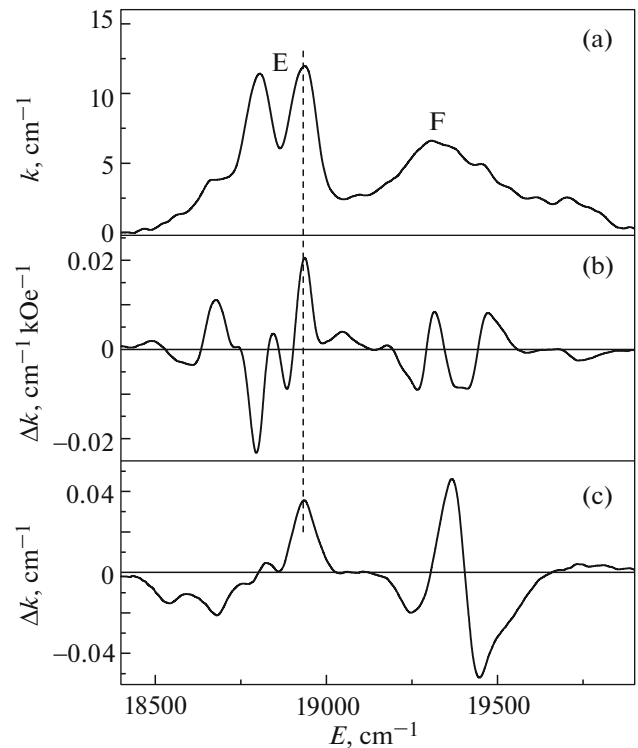
field, $c = (k_{m+} + k_{m-})/k_m$ is the paramagnetic MOA of the transition, $\Delta\omega_0$ is the Zeeman splitting of the line, and $\varphi(\omega, \omega_0)$ is the shape function of the absorption line. For states with a half-integer moment, the paramagnetic mixing term (B-term) may be neglected. From the comparison of the experimental spectra presented in Figs. 1−5 with formula (1), it is evident that the fine structure of the spectra is caused by the diamagnetic effect, but we are interested in the integral paramagnetic effect. On the integration of (1) for both one absorption line and a band consisting of several lines, the diamagnetic effect yields zero; therefore, for the integral MOA, we can write

$$c = \frac{\langle \Delta k(\omega) \rangle_0}{\langle k(\omega) \rangle_0} = C \frac{\mu_B H}{k_B(T - \theta)}. \qquad (2)$$

Here, we have taken into account that, according to van Vleck and Hebb [26], the MOA should be proportional to the paramagnetic susceptibility and that the susceptibility obeys the Curie−Weiss law in the considered temperature interval. If this is true, then the dimensionless parameter C should be independent of temperature. Relationship (2) was experimentally confirmed with the help of the Faraday effect, which, in the transparency band of the material, is caused by

The MOA (*C*) and NOA (*A*) of transitions at room temperature

Notation	Transition	λ, nm	E, cm^{-1}	C (experiment)	A, 10^{-4} (experiment)
R	$^4I_{9/2} \to {}^4F_{3/2}$	880	11400	+2.62	−27
S	$^4I_{9/2} \to {}^2H_{9/2} + {}^4F_{5/2}$	800	12400	+0.22	−7.7
A	$^4I_{9/2} \to {}^4S_{3/2} + {}^4F_{7/2}$	750	13500	−1.94	−5.3
D	$^4I_{9/2} \to {}^2G_{7/2} + {}^4G_{5/2}$	590	16800	+2.2	−10.7
E	$^4I_{9/2} \to {}^2K_{13/2} + {}^4G_{7/2}$	530	18900	+0.95	−3.6
F	$^4I_{9/2} \to {}^4G_{9/2}$	515	19500	−1.13	−15.5

allowed transitions in the ultraviolet band. The aim of the present work is to check the situation with forbidden *f–f* transitions.

The paramagnetic susceptibility of $Nd_{0.5}Gd_{0.5}Fe_3(BO_3)_4$ obeys the Curie–Weiss law in the considered temperature range with the Weiss parameter along the axis C_3 of $\theta_C = -45$ K. From the absorption and MCD spectra (Figs. 1−5) with the help of relationships (2), the parameters C were found (see Fig. 7 and the table). They proved to be temperature-dependent. The reason of this phenomenon was earlier explained in detail in our works [9, 12]. Let us outline the main ideas.

The parity-forbidden *f–f* transitions are partly allowed due to the admixture of states of the opposite parity with odd components of the crystal field (both static and dynamic). Assume that high-energy states with opposite parity J'_F are admixed only to the excited 4*f* state (J_F), because they are closer to it. In this case, the transition will be partly allowed if the admixed

state J'_F satisfies the selection rule with respect to the total moment:

$$|J'_F - J_I| \le 1, \qquad (3)$$

where J_I is the total moment of the ground state. Thus, the *f–f* transitions from the ground state ($^4I_{9/2}$ for Nd^{3+} ions) with $J = 9/2$ become partly allowed due to the admixing of states with $J = 7/2$, 9/2, and 11/2. The allowed transitions from the ground state to these admixtures determine not only the intensity of absorption, but also the MOA of the transition. This problem was solved in [9, 12] in the free-atom approximation. This approximation is valid in the case of a high population of all components of splitting of the ground state by the crystal field. Therefore, the table presents the MOA of transitions at the maximum temperature. The following results were theoretically obtained:

for transition $J \to (J-1)$ $C = -g(J+1)/2 = -2,$

for transition $J \to J$ $C = -g/2 = -0.36,$ (4)

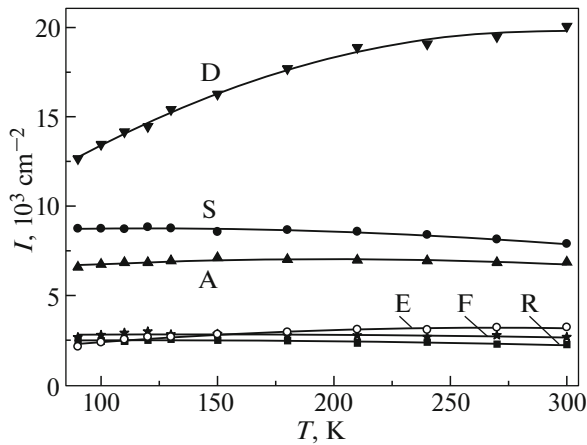for transition $J \to (J+1)$ $C = +gJ/2 = +1.64.$

Fig. 6. Temperature dependences of the intensities of absorption bands.
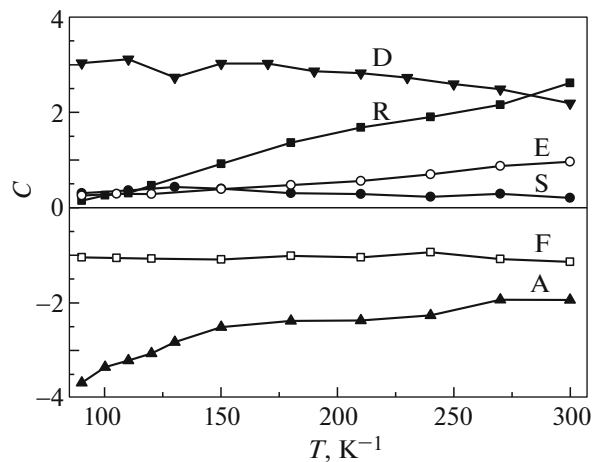

Fig. 7. Temperature dependences of the MOA of absorption bands.

Here, g is the Lande parameter of the ground state. It is evident from the table that the MOA of the f–f transitions under study lie approximately within theoretically possible values (4). Comparing the experimental MOA (see table) with theoretical ones, we can estimate the state the admixture of which allows the transition. In particular, the MOA of the R and D transitions are determined by the admixture of the state with $J = 11/2$. If the absolute value of the parameter C at room temperature is smaller than the maximum possible one, this means that there are at least two contributions (4) to the MOA.

The Jadd−Ofelt theory, which describes the allowance of the f–f transitions, gives the following selection rule for these transitions [27]:

$$|J_F - J'_F| \le \lambda. \tag{5}$$

Here, $\lambda = 2$, 4, and 6 for the $4f$ shell. All considered transitions satisfy these conditions. From (3) and (5), we find that the admixed states should satisfy the condition

$$|J_F - J'_F| \le \lambda - 1. \tag{6}$$

It is easy to check that all the considered transitions are allowed by all three admixtures to the excited state.

The splitting of the $4f$ state by the crystal field is rather strong. In particular, the splitting of the ground state of the Nd^{3+} ion in $NdFe_3(BO_3)_4$ equals 322 cm^{-1} (463 K) [28]. With variation in temperature, the population of the components of splitting of the ground state changes. This can lead to the change in the relationship between three contributions (4) to the MOA and, therefore, to deviation of the temperature dependence of the MOA from the Curie−Weiss law and of the parameter C from a constant, which is observed in the experiment (Fig. 7).

It is especially worth noting that the increase in the absolute value of the parameter C with a decrease in temperature substantially exceeds its theoretical values (4) (bands A and D in Fig. 7). It is known that, in uniaxial crystals, the electron states of an atom split in the first approximation in accordance with the absolute value of M_J, as well as in a uniform electric field. In [9], it was shown that the MOA of the transition from the state $M_J = J$, the population of which increases with a decrease in temperature, exceeds the values (4) two-fold.

The symmetry of the $Nd_{0.5}Gd_{0.5}Fe_3(BO_3)_4$ crystal has no center of inversion; therefore, the NCD can exist in it. Indeed, the NCD was detected and measured. The presence of the NCD also demonstrates that the number of opposite inverse twins is not the same. The NCD spectra are presented in Figs. 1−5. According to relationship (1), the MCD spectra are caused by splitting in the magnetic field and qualitatively repeat the derivative of the absorption spectra (Figs. 1−5). The NCD spectra qualitatively repeat the absorption spectra that characterize the splitting of the
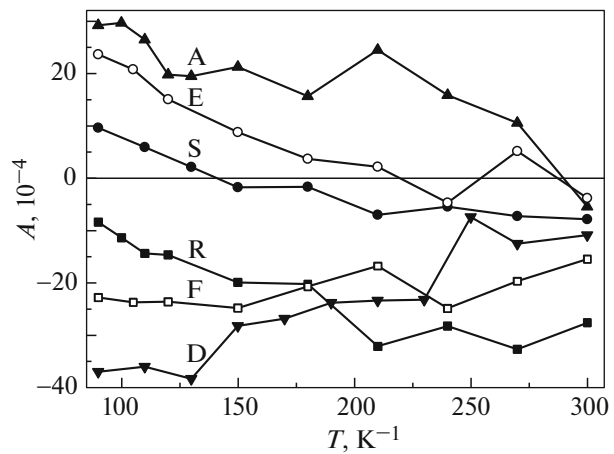

Fig. 8. Temperature dependences of the NOA of absorption bands.

$4f$ states by a crystal field. However, the NCD can have different signs and, therefore, can be sensitive to small splitting in the crystal field. An example of such a situation is presented in Fig. 3. The NCD spectrum at room temperature indicates the splitting of the absorption line near 13 500 cm^{-1}, which is not directly seen in the absorption spectrum. At low temperatures, indeed, two close lines are observed in this region. The NCD spectrum at 90 K (Fig. 3) also manifests these lines directly. It should be noted that the comparison of the NCD spectra at two temperatures demonstrates the change in the sign of the NCD of one of the lines with the variation in temperature.

The integral NOA of the transition is described by the relationship

$$A = \frac{R_{if}}{D_{if}} \approx \frac{\langle \Delta k \rangle_0}{\langle k \rangle_0}, \tag{7}$$

where k is the absorption coefficient and Δk is the NCD. This quantity differs by the coefficient 0.25 from the "anisotropy factor" employed in other works. The integral values of the NCD of the transitions were found from the spectra presented in Figs. 1−5. The obtained temperature dependences of the NOA are presented in Fig. 8. From the comparison of the NCD and absorption spectra (Figs. 1−5) and the integral NOA (Fig. 8), we see that the NOA of separate lines significantly exceeds (approximately by an order of magnitude) the integral NOA bands, due to the variable sign of the NCD.

According to [29], the rotation force R_{if} is defined as

$$R_{if} = \text{Im}[\langle i|\mathbf{d}|f \rangle \langle f|\mathbf{m}|i \rangle], \tag{8}$$

where $\mathbf{d}$ and $\mathbf{m}$ are the electric and magnetic dipole moments, respectively. The dipole force is $D_{if} = |\langle i|\mathbf{d}|f \rangle|^2$, because the transitions under consideration mostly have an electric dipole nature. However, according to (8), for the existence of NCD, the matrix

element of the magnetic dipole moment of the transition should also be nonzero. Indeed, taking into account the mixing of terms by the spin-orbital interaction in the first approximation of the perturbation theory and the mixing of states of the same symmetry by the crystal field, all transitions under consideration are allowed in the magnetic-dipole approximation. The NOA of the allowed transition are independent of temperature. However, the NOA values of the forbidden *f–f* transitions essentially depend on temperature (Fig. 8) up to the change of the sign. The nature of this phenomenon is similar to that described above for the MOA of the *f–f* transitions. The integral NOA also consists of three contributions, corresponding to three contributions to the allowance of the *f–f* transitions. Unfortunately, the theoretical value of these contributions are unknown and cannot be known, because the contributions to the absorption and MCD were calculated in the free-ion approximation, but the NCD in a free ion is absent. At the same time, from the experimental results (Fig. 8), it is evident that these contributions have different signs, as in the case of MOA. The integral intensities of the *f–f* absorption bands depend on temperature significantly more weakly than the MOA and NOA (Fig. 6–8), because the three contributions to absorption have the same signs, but the contributions to the MOA and NOA are of different signs. In contrast to the MCD, the NCD can exist only in not centrally symmetric crystals. Therefore, the stronger temperature dependence of the NOA than the temperature dependence of the MOA (Figs. 7 and 8) may indicate locally not centrally symmetric distortions of the crystal in the corresponding excited states. The strong variation in the NOA of the *f–f* transitions with temperature makes problematic the analysis of the geometry of the neighborhood of the 4*f* ion on the basis of the NOA of the *f–f* transitions at one temperature.

4. CONCLUSIONS

On the basis of the measured absorption, MCD, and NCD spectra of the *f–f* transitions in the Nd^{3+} ion in the $Nd_{0.5}Gd_{0.5}Fe_3(BO_3)_4$ crystal at different temperatures, temperature dependences of the MOA and NOA of the transitions have been obtained. It has been found that, in contrast to allowed transitions, the variation in the MOA of the *f–f* transitions does not obey the Curie–Weiss law and the NOA depends on temperature. Moreover, the NOA of some transitions changes sign with variation in temperature. These phenomena are the result of the presence of three contributions to the allowance of the *f–f* transitions, which lead to three contributions to the MOA and NOA with different signs. The theoretical model made it possible to predict the range of the MOA of the *f–f* transitions in the Nd^{3+} ion, and the experiment has confirmed these conclusions. The strong variation in the NOA of the *f–f* transitions with temperature makes problematic the analysis of the geometry of the neighborhood of the 4*f* ion on the basis of the NOA of the *f–f* transitions at one temperature.

REFERENCES

1. Y. K. Zhou, S. Emura, S. Hasegawa, and H. Asahi, Phys. Status Solidi C **8** (7−8), 2173 (2011).
2. C. Bonardi, R. A. Carvalho, H. C. Basso, M. C. Terrile, G. K. Cruz, L. E. Bausa, and J. Garcia Sole, J. Chem. Phys. **111**, 6042 (1999).
3. H. De Leebeeck, K. Binnemans, and C. Görller-Walrand, J. Alloys Compd. **291**, 300 (1999).
4. I. Couwenberg and C. Gorller-Walrand, J. Alloys Compd. **275−277**, 388 (1998).
5. K. Binnemans, D. Verboven, C. Gorller-Walrand, J. Lucas, N. Duhamel-Henry, and J. L. Adam, J. Alloys Compd. **250**, 321 (1997).
6. L. Fluyt, E. Hens, H. De Leebeeck, C. Gorller-Walrand, and K. U. Leuven, J. Alloys Compd. **250**, 316 (1997).
7. I. V. Ignat'ev and V. V. Ovsyankin, Opt. Spectrosc. **76** (6), 862 (1994).
8. A. V. Malakhovskii, A. L. Sukhachev, V. V. Sokolov, T. V. Kutsak, V. S. Bondarev, and I. A. Gudim, J. Magn. Magn. Mater. **384**, 255 (2015).
9. A. V. Malakhovskii, A. L. Sukhachev, A. Yu. Strokova, and I. A. Gudim, Phys. Rev. B: Condens. Matter **88**, 075103 (2013).
10. A. V. Malakhovskii, U. V. Valiev, I. S. Edelman, A. E. Sokolov, I. Yu. Chesnokov, and I. A. Gudim, Opt. Mater. **32**, 1017 (2010).
11. A. V. Malakhovskii, I. S. Edelman, A. L. Sukhachev, V. V. Markov, and V. N. Voronov, Opt. Mater. **32**, 243 (2009).
12. A. V. Malakhovskii, V. A. Isachenko, A. L. Sukhachev, A. M. Potseluiko, V. N. Zabluda, T. V. Zarubina, and I. S. Edel'man, Phys. Solid State **49** (4), 701 (2007).
13. L. Alyabyeva, V. Burkov, O. Lysenko, and B. Mill, Opt. Mater. **34**, 803 (2012).
14. D. Shirotani, H. Sato, K. Yamanari, and S. Kaizaki, Dalton Trans. **41**, 1057 (2012).
15. V. I. Burkov, O. A. Lysenko, and B. V. Mill, Crystallogr. Rep. **55** (6), 983 (2010).
16. V. I. Burkov, A. V. Butashin, E. V. Fedotov, A. F. Konstantinova, and I. A. Gudim, Crystallogr. Rep. **50** (10), 954 (2005).
17. V. I. Burkov, A. V. Egorysheva, A. Ya. Vasil'ev, Yu. F. Kargin, and V. M. Skorikov, Inorg. Mater. **38** (10), 1035 (2002).

18. L. Fluyt, I. Couwenberg, H. Lambaerts, K. Binnemans, and C. Görller-Walrand, J. Chem. Phys. **105**, 6117 (1996).

19. A. M. Kadomtseva, Yu. F. Popov, G. P. Vorob'ev, A. A. Mukhin, V. Yu. Ivanov, A. M. Kuz'menko, A. S. Prokhorov, L. N. Bezmaternykh, V. L. Temerov, and I. A. Gudim, in *Proceedings of the XXI International Conference "New in Magnetism and Magnetic Materials," Moscow, June 28–July 4, 2009*, p. 316.

20. A. V. Malakhovskii, E. V. Eremin, D. A. Velikanov, A. V. Kartashev, A. D. Vasil'ev, and I. A. Gudim, Phys. Solid State **53** (10), 2032 (2011).

21. A. V. Malakhovskii, A. L. Sukhachev, A. A. Leont'ev, I. A. Gudim, A. S. Krylov, and A. S. Aleksandrovsky, J. Alloys Compd. **529**, 38 (2012).

22. A. V. Malakhovskii, S. L. Gnatchenko, I. S. Kachur, V. G. Piryatinskaya, A. L. Sukhachev, and V. L. Temerov, J. Magn. Magn. Mater. **375**, 153 (2015).

23. A. V. Malakhovskii, S. L. Gnatchenko, I. S. Kachur, V. G. Piryatinskaya, A. L. Sukhachev, and I. A. Gudim, J. Alloys Compd. **542**, 157 (2012).

24. A. D. Balaev, L. N. Bezmaternykh, I. A. Gudim, V. L. Temerov, S. G. Ovchinnikov, and S. A. Kharlamova, J. Magn. Magn. Mater. **258**−**259**, 532 (2003).

25. A. V. Malakhovskii, A. L. Sukhachev, A. D. Vasil'ev, A. A. Leont'ev, A. V. Kartashev, V. L. Temerov, and I. A. Gudim, Eur. Phys. J. B **85**, 80 (2012).

26. J. H. Van Vleck and M. H. Hebb, Phys. Rev. **46**, 17 (1934).

27. R. D. Peacock, Struct. Bonding (Berlin) **22**, 83 (1975).

28. M. N. Popova, E. P. Chukalina, T. N. Stanislavchuk, B. Z. Malkin, A. R. Zakirov, E. Antic-Fidancev, E. A. Popova, L. N. Bezmaternykh, and V. L. Temerov, Phys. Rev. B: Condens. Matter **75**, 224435 (2007).

29. W. Moffit and A. Moscovitz, J. Chem. Phys. **30**, 648 (1959).

Translated by E. Chernokozhin